Environmental Science Nano

ROYAL SOCIETY OF CHEMISTRY

PAPER

View Article Online
View Journal | View Issue

Cite this: *Environ. Sci.: Nano*, 2025, 12, 3699

The sulphidation of ZnO nanoparticles enhances zinc recovery in Zn-starved barley (*Hordeum vulgare* L.): the interplay of metal acquisition and cellular homeostasis†

Izabela Jośko, *[a] Mikołaj Feculak,[a] Patryk Oleszczuk,[b] Bożena Czech,[b] Mohammed Alyafei,[c] Magdalena Sozoniuk [a] and Mohamed Sheteiwy[c]

The sulphidation of metal-based engineered nanoparticles (ENPs) presents a promising strategy to alleviate their ecotoxicity, particularly for ZnO ENPs used in plant growth enhancement. However, little is known about the interactions of sulphidized ENPs with plants, including their ionome. The key properties of ENPs that drive plant growth improvement can be significantly impacted by sulphidation. This study investigated the response of Zn-deficient barley to pristine (nZnO) and sulphidized ZnO ENPs (sulph-nZnO) at 0.5 mg_{Zn} L^{-1} under hydroponic conditions. The experimental approach evaluated plant biomass, elemental composition, and gene expression related to metal acquisition and homeostasis. Key findings revealed that Zn treatment of Zn-deficient plants showed higher Zn loading than the plants grown with the Zn source by 43–117%, and Zn distribution was primarily concentrated in shoots, in which the Zn level was as follows: nZnO < sulph-nZnO < $ZnSO_4$. ENPs caused a comparable accumulation pattern of other metals (Fe, Mn, K, Ca) in barley shoots after 7 days, and their content was higher than $ZnSO_4$ treatment. The transcript levels of most of the analyzed ZIP genes were similar regardless of the Zn compound treatments. In contrast, the gene expression related to vacuolar Zn sequestration and antioxidant mechanisms exhibited variability in the Zn-treated plants. In turn, the expression patterns of genes encoding Zn sequestration and antioxidant enzymes in barley shoots and roots did not directly correlate with total Zn content in plant tissues. However, the distinct transcriptional response may be associated with the ratios of different metals present. Although the spectroscopic and transcriptional profiles were generally consistent across ENP treatments, sulph-nZnO exhibited enhanced Zn uptake and elevated expression of *ZIP1*, a zinc-responsive gene involved in zinc efficiency. This suggests its potential as an innovative approach to improving plant elemental nutrition.

Received 12th December 2024,
Accepted 20th May 2025

DOI: 10.1039/d4en01165a

rsc.li/es-nano

Environmental significance

Taking into account that ENPs, designed to enhance plant growth, may induce adverse effects on biota, there is a pressing need to develop safer and more efficient nano-enabled agrochemicals. The study revealed that sulphidized ZnO ENPs lead to higher Zn and transition metal uptake in Zn-starved barley compared to pristine ENPs, despite similar Zn release rates. Nonetheless, the pattern of evaluated traits indicated that both types of ENPs were similar to Zn-sufficient plants, yet distinctly different from Zn^{2+} exposure. The findings unveil that sulphidation by altering the properties of ENPs enhances their potential for promoting plant growth and nutritional value.

1. Introduction

Zn is an essential element for plant growth and development that serves as a cofactor for a broad range of enzymes, such as copper/zinc superoxide dismutase, and as a structural component of proteins, including zinc-finger domain proteins.[1] These biomolecules are integral to various biological processes, including transcription, translation, photosynthesis, hormone regulation, and plant immunity.[1]

[a] *Institute of Plant Genetics, Breeding and Biotechnology, Faculty of Agrobioengineering, University of Life Sciences, 20-950 Lublin, Poland. E-mail: izabela.josko@up.lublin.pl; Fax: +48 81 4456031; Tel: +48 81 4456675*
[b] *Department of Radiochemistry and Environmental Chemistry, Faculty of Chemistry, Maria Curie-Skłodowska University, 20-031 Lublin, Poland*
[c] *Department of Integrative Agriculture, College of Agriculture and Veterinary Medicine, United Arab Emirates University, P.O. Box 15551, Al Ain, Abu Dhabi, United Arab Emirates*

† Electronic supplementary information (ESI) available. See DOI: https://doi.org/10.1039/d4en01165a

However, it is estimated that approximately 50% of agricultural soils worldwide are affected by either a deficiency or limited bioavailability of Zn.[2] This leads to Zn starvation in plants, with subsequent implications for human nutrition, as approximately one-third of the global population is projected to be affected by inadequate Zn intake.[2] To combat Zn shortage, Zn fertilization, involving either soil amendment or foliar application, is a commonly employed strategy in crop production.[3] It is noteworthy, however, that approximately 50% of the applied nutrients do not reach their intended targets. This results in substantial losses of the active ingredient and contributes to both soil and groundwater pollution.[4]

The advancement of nanotechnology unveils novel opportunities across various economic sectors, including agriculture.[5] Due to their nano-scale diameter (1–100 nm) and significantly increased surface area, engineered nanoparticles (ENPs) exhibit unique physicochemical properties, rendering them more efficient than their bulk counterparts when using traditional nano-agrochemicals.[3] The superiority of metal-based ENPs over their micro-sized counterparts is attributed to their gradual release of metal ions and enhanced capability to cross biological barriers due to their particle size.[3] These attributes contribute to an increase in the efficacy of nano-chemicals, which, in turn, facilitates a reduction in material losses and minimizes the potential for environmental contamination. Nowadays, it is of key importance in the face of the "from farm to fork" strategy implemented by the European Commission, mandating at least 50% and 20% reductions in nutrient loss and fertilizer use by 2030.[6]

Zn-based ENPs are among the most frequently employed nanomaterials to boost plant growth, serving as fertilizers or stimulants of plant defense mechanisms.[7] The positive effects of ZnO ENPs on plants, especially when applied in low concentrations, have been documented in multiple studies across diverse plant species and growth conditions.[3,4] However, due to their classification as a class B soft metal, ZnO ENPs exhibit higher solubility compared to other nanoparticles like Ag or Cu.[8] As a result, the extended studies have noted comparable effects between ZnO ENPs and Zn ions.[9,10] In pursuit of this objective, efforts are being made to enhance the efficiency and safety of ENPs.[5] The sulphidation of ENPs, which can occur in sulfur-rich environments such as sewage sludge, has primarily been examined concerning environmental fate and ecotoxicity.[11–13] Given the frequently observed reduced harmful impact of sulphidized ENPs compared to their pristine counterparts,[13,14] it has been postulated that sulphidation could be a viable strategy for reducing the toxicity of metal-based ENPs[14] while maintaining the activity of the metal core.

There is limited knowledge regarding the interactions between sulphidized ENPs and edible plants. Considering the altered properties of ZnO ENPs following sulphidation – such as particle size, chemical composition, and solubility[11] – it is highly probable that plant responses will also be affected. Sulphidized Ag ENPs evoked distinct patterns of uptake and distribution of Ag in *Brassica rapa* compared to the pristine ENPs and metal ions.[15] Correspondingly, a comparable accumulation of Ag was noted in the aquatic plant *Landoltia punctata* after 24 hours of exposure to pristine and sulphidized Ag ENPs.[13] However, data on the impact of sulphidized ZnO ENPs on plants remains underexplored. Additionally, there is a knowledge gap involving the evaluation of effects induced by ENPs under Zn-deficient conditions. Typically, both the growth-promoting and ecotoxicological effects of Zn-based ENPs on plants have been assessed in Zn-efficient media and at relatively high concentrations of ENPs.[16–18] Meanwhile plants growing under micronutrient deficiencies employ various strategies for growth, such as medium acidification, the release of complexing agents, and delayed root suberization, which may subsequently influence ENP uptake.[19,20] Further, to maintain metal balance under different Zn regimes, plants have developed sophisticated mechanisms regulating metal balance, including zinc-regulated transporters, iron-regulated transporter-like protein (ZIP) transporters, and metal tolerance/transport protein (MTP).[21] Therefore, the changes in gene expression related to metal homeostasis serve as valuable markers of zinc nutritional status in plants.[1,7] Recently, the transcripts of metal transporters have been more frequently analyzed in plants exposed to metal-based ENPs.[17,22–24] Because the effects of pristine ENPs have been studied in metal-sufficient plants and/or at high doses, resulting in excessive responses, there remains a lack of understanding about the efficiency of Zn when ENPs are administered at the required dose for the target element.

This study aimed to determine the zinc efficiency of hydroponically grown barley (*Hordeum vulgare* L.) subjected to zinc-deficient conditions, following the application of pristine and sulphidized ZnO ENPs at a specified concentration. The research involved analyzing Zn content in both root and shoot tissues. Furthermore, gene expression analysis was performed on genes directly related to metal homeostasis to evaluate the Zn cellular status of the plants. It was hypothesized that alterations in the properties of ZnO ENPs due to sulphidation would modulate Zn loading and elemental composition in plants, thereby producing effects distinct from those observed with pristine ENPs and Zn^{2+}. The findings obtained from this study are expected to expand the understanding of the interactions between sulphidized ENPs and plants, which is valuable for both agricultural and environmental applications. Specifically, this information could be instrumental in designing nano-tuned agrochemicals and potentially replacing conventional agents with more efficient formulations that have less environmental impact.

2. Materials and methods

2.1. Sulphidation of ZnO ENPs

ZnO ENPs (nZnO) as powder were purchased from Sigma Aldrich (cat no. 544906). The particle size of pristine nZnO

was less than 100 nm. nZnO was sulphidized following the method by Li *et al.*[14] In brief, a 0.001 M $Na_2S_9H_2O$ solution (POCH, Poland) was introduced into a 0.01 M $NaNO_3$ solution (POCH, Poland), followed by sonication for 10 minutes. Subsequently, the quantity of nZnO was added to achieve different S: ZnO ratios as shown in Table S1 (ESI†). The sulphidation process was conducted at room temperature under continuous stirring conditions (48 hours at 120 rpm). Then the suspensions were centrifuged (9000*g* for 30 minutes), the pellet was washed with ultrapure water, and air-dried at room temperature to obtain the solid sulphidized particles. The highest conversion rate of ZnO to ZnS form nanoparticles (87.7%) was subsequently utilized for further studies and called "sulph-nZnO".

2.2. Characterization of the pristine and sulphidized ENPs

The pristine and sulphidized ZnO ENPs powders were characterized by properties crucial for their behavior and interactions with plants. Transmission electron microscopy determined the morphology and average particle size with energy-dispersive X-ray spectroscopy (TEM-EDS; Titan G2 60e300, FEI). The BET surface area (S_{BET}) and porosity (pore volume, micropore volume) were measured by N_2 adsorption–desorption studies (ASAP Quantachrome Micromeritics Inc.), and surface composition by X-ray photoelectron spectroscopy (XPS; UHV Prevac). The ζ-potential and the size of aggregates of nZnO and sulph-nZnO were assessed using the Dynamic Light Scattering (DLS) technique (Zetasizer 3000, Malvern, UK).

The properties of the pristine and sulphidized ZnO ENPs were described in detail in previous work.[11] As confirmed by XPS analysis, nZnO was incompletely transformed into ZnS nanoparticles during the sulphidation process (Table S1 and Fig. S1†). The XPS spectra indicated that sulfur (1%) was completely bonded as ZnS. This was corroborated by S 2p 3/2 peaks observed at 162 eV. Sulph-nZnO exhibited nearly two times higher specific surface area than nZnO (Table S2†). The obtained sulph-nZnO is characterized by a well-developed mesoporous structure based on the IUPAC classification. After sulphidation, the pore volume and pore radius of nZnO increased by factors of 8 and 3, respectively. TEM images (Fig. 1) showed that the sulphidation of nZnO resulted in the reduction of the grain size: the average particle sizes of nZnO and sulph-nZnO were measured at 52.8 nm and 11.8 nm, respectively. Furthermore, the change in the particle morphology was observed after sulphidation, forming ZnS particles characterized by spherical-like shape, while the pristine nZnO particles were spherical or rod-shaped. Sulph-nZnO exhibits a shell/core structure, which was due to the dissolution of ENPs and the subsequent precipitation of ZnS on the ZnO ENPs. The reduced grain size after sulphidation probably prompts the higher aggregation of sulph-nZnO. The DLS analysis determined a 30% bigger aggregate of sulph-nZnO compared to nZnO (1646 nm).

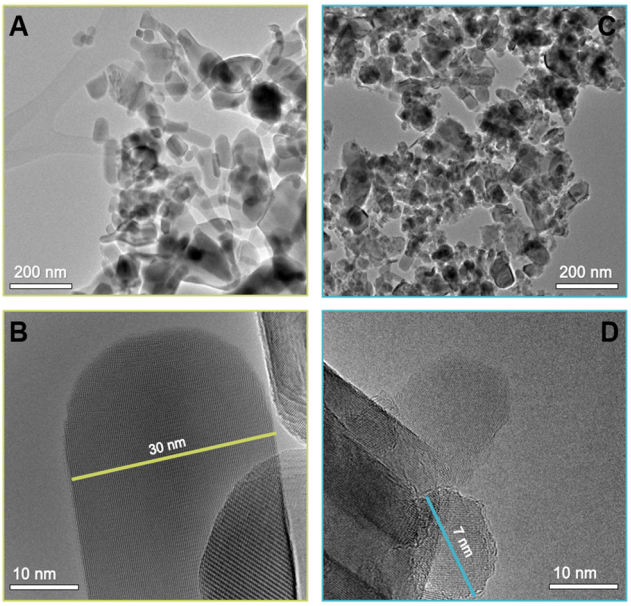

Fig. 1 TEM images of nZnO (A and B) and sulph-nZnO (C and D).

2.3. Plant growth and exposure to ZnO ENPs and Zn^{2+}

Hordeum vulgare L. cultivar Ella seeds were initially soaked for 2 hours in Milli-Q® water. The seeds then underwent a surface sterilization process involving immersion in 2% calcium hypochlorite for 15 minutes, followed by a brief exposure to 70% ethanol for 1 minute. Post-sterilization, the seeds were thoroughly rinsed three times with Milli-Q® water to remove residual sterilizing agents. These sterilized seeds were placed on Petri dishes lined with filter paper that was saturated with Milli-Q® water to initiate germination. The Petri dishes were then placed in a growth chamber maintained at a temperature of 24 °C and kept in the dark. After 4 days, the germinated seedlings were transferred to a nutrient solution containing a modified Hoagland's solution (HGL), composed of the following elements: 0.457 mM $MgSO_4{\cdot}7\ H_2O$, 1 mM KNO_3, 0.1 mM KH_2PO_4, 1 mM $Ca(NO_3)_2$, 0.0336 mM $NaSiO_3{\cdot}5\ H_2O$, 1 μM $Mo_7O_{24}(NH_4)_6$, 0.06 mM NaFe(III) EDTA, 1 μM $MnCl_2$, 3 μM H_3BO_3, and 0.2 μM $CuSO_4$ buffered with 2 mM MES (4-morpholineethanesulfonic acid, 2-(*N*-morpholino) ethanesulfonic acid hydrate)-KOH, without the addition of a Zn source (pH = 6.6 ± 0.3). The group of plants growing in the Hoagland solution without a Zn source was referred to as the control (−). One group of seedlings was cultivated in Hoagland solution containing 1 μM $ZnSO_4$ $7H_2O$, serving as the positive control, and referred to as the control (+). The pH of Hoagland's solution with Zn ions was unchanged, as in the Zn-free solution. The hydroponic solutions were refreshed weekly with a fresh medium and were continuously aerated to maintain optimal oxygenation. The plants were grown under hydroponic conditions within a growth chamber (Conviron GEN1000) set to a relative humidity of 60 ± 10%, with a light/dark cycle of 16 hours/8 hours. The chamber temperatures were maintained at 23 ± 3 °C during the day and 18 ± 3 °C at night.

Three-week-old plants, at the onset of the tillering stage (BBCH: 21), were exposed to nZnO/sulph-nZnO/$ZnSO_4$ by introducing them to a Zn ion-free Hoagland medium (Table S3†). These compounds were applied at a concentration of 0.5 mg of Zn per liter by molar weight. The used rate corresponds to 1 μM $ZnSO_4$ $7H_2O$ used for Zn-sufficient Hoagland solutions. The solutions were subjected to sonication in an ultrasonic bath at 25 °C, with settings of 250 W and 50 Hz, for 30 minutes. Plants were harvested for analysis 1 and 7 days following treatment. Fresh flag leaves and roots were collected for the transcriptional analysis. Plant tissues for the metal content analysis were rinsed with Milli-Q® water to ensure cleanliness. To effectively remove any nano-Zn adhering to the root surfaces, the roots underwent an additional rinse with 2.2 M HNO_3 for 30 seconds, followed by three rinses with Milli-Q® water. Part of the roots after etching was also collected for the microscopic analysis with Scanning Electron Microscopy (SEM) integrated with Energy Dispersive Spectroscopy (EDS) (Quanta™ 3D FEG, FEI with EDAX SDD Apollo detector) to assess the efficiency of the etching protocol. The plant samples were subsequently air-dried, weighed, and stored in the dark at 20 °C to facilitate elemental composition analysis.

2.4. Characteristics of ENP solutions

The ENPs in the HGL solution were characterized for ζ-potential, aggregate size, and dissolution rate immediately after being added to the solutions and subjected to sonication, just before plant exposure. The ζ-potential and the particle size distribution of nZnO and sulph-nZnO in HGL solution were assessed using the Dynamic Light Scattering (DLS) technique (Zetasizer 3000, Malvern, UK). To separate the dissolved Zn from the solution, ultrafiltration was performed using Microsep Advance centrifugal devices with omega membrane 1 K (Pall Corporation). Next, the concentration of Zn ions in the filtered solutions was measured with an Inductively Coupled Plasma Optical Emission Spectrometer (ICP-OES, Thermo Fisher Scientific, iCAP 7200, USA). An axial configuration and a spectral line at 206.200 nm were selected for Zn measurements to maximize sensitivity and minimize interference.

2.5. Medium analysis post-harvesting of plants

The plants of the growth medium underwent characterization *ad hoc* after removing the plants. pH and electrolytic conductivity (EC) measurements were conducted using a pH/conductivity meter CPC-505 (Elmerton, Poland). The dissolved organic carbon (DOC) and total organic carbon (TOC) were quantified with a Shimadzu SSM-5000A analyzer. The concentration of zinc ions was determined as detailed in the preceding section (2.4).

2.6. Determination of micro- and macroelements in plant tissues

Dried plant tissues (roots and shoots) were digested using a $HNO_3 : H_2O_2$ (4 : 1) mixture within Teflon vessels, utilizing a microwave oven (Milestone, ETHOS EASY, Italy) for 1 hour at a temperature of 200 °C. Following the cooling process, the samples underwent filtration through a 0.45 μm PTFE filter and were subsequently diluted with Milli-Q® water to a final volume of 25 mL for analysis *via* ICP-OES (iCAP 7200). Each analysis incorporated blank samples. For quality control of the digestion process, certified reference material (tomato leaves, NIST® SRM® 1573a) was employed, undergoing digestion identical to that of the barley samples. The recovery rates for selected microelements and macroelements were within the ranges of 93.6–98.4% and 89.3–94.8%, respectively. The recovery was assessed by analyzing the results obtained from the digested certified reference material (tomato leaves, NIST® SRM® 1573a) and comparing them with the element levels specified in the certificate.

2.7. Analysis of gene expression in plants

To analyze gene expression, the total RNA was extracted from the flag leaves and roots of *H. vulgare* (~50 mg) utilizing the TRIzol™ reagent (Invitrogen, USA), per the manufacturer's guidelines. The extraction process was conducted in three biological replicates. RNA was quantified using a NanoDrop 2000 spectrophotometer (Thermo Scientific). The quality and integrity of the RNA were assessed *via* 2% agarose gel electrophoresis stained with ethidium bromide. To eliminate genomic DNA, the RNA was treated with RNase-free DNase I (Thermo Scientific). Reverse transcription was executed in 20 μL reactions containing 1 μg of RNA, employing the NG dART RT kit (EURx) in line with the manufacturer's instructions. The resulting cDNA (50 ng μL^{-1}) served as the template for qPCR analysis.

Real-time qPCR analysis was performed to quantify the transcript levels of genes within the Zn-regulated, iron-regulated transporter-like protein (ZIP) family (*ZIP1, 3, 6, 8, 10, 14*), the metal tolerant protein (MTP) family (*MTP1*), and the gene encoding superoxide dismutase (*SOD Cu-Zn*). These genes are associated with Zn homeostasis in plants (*ZIP1, ZIP3, ZIP6, ZIP8, ZIP10, ZIP14, MTP1*) and defense against oxidative stress (*SOD Cu-Zn*) and localized in different cellular compartments (Table S4†). Two genes – actin (ACT) and ADP-ribosylation factor 1 (ADP) – were selected as internal controls for data normalization. Gene-specific primers were either sourced from the existing literature or designed using OligoArchitect™ Online (Sigma-Aldrich), as elaborated in the ESI† (Table S4). Real-time qPCR reactions were performed using PowerUp™ SYBR™ Green Master Mix (Applied Biosystems) according to the manufacturer's protocols, with a total reaction volume of 20 μL for 10 ng of template cDNA and 500 Nm of primer concentration. The cycling protocol included: for 2 minutes at 50 °C, for 2 minutes at 95 °C, followed by 40 cycles of 15 seconds at 95 °C, and for 1

minute at 60 °C. Reactions were executed in three biological and three technical replicates, inclusive of a no-template control. Standard curves derived from five dilution points were utilized to ascertain the amplification efficiency for each primer pair. All real-time qPCR reactions were conducted on the QuantStudio™ 3 Real-Time PCR System (Applied Biosystems™). Data analysis was performed using the relative quantification software module from ThermoFisher Cloud (ThermoFisher Scientific), and relative gene expression was determined using the $2^{-\Delta\Delta Ct}$ method.

2.8. Statistical analysis

All statistical analyses were conducted using OriginPro 2023 software. Differences between treatments were assessed through a one-way analysis of variance (ANOVA), followed by Tukey's or Dunnett's *post hoc* tests, with a significance level set at 0.05. Additionally, cluster analysis was utilized to evaluate the similarity of plant response patterns across different treatments. Principal components analysis (PCA) was performed to summarize the similarities and differences among all sample groups. The correlation plots based on the two-tailed Pearson factors were constructed to test variables. To characterize the impact of treatments on plant growth and metal distribution, the relative growth rate (RGR) and the translocation factor (TF) were calculated. RGR, the rate of increase of total dry weight measured during the time exposure (7 days), was calculated according to the following equation:

$$RGR = DW_2 - DW_1/t_2 - t_1 \quad (1)$$

where DW (mg) – the dry matter of different plant tissues (shoots and roots) and the whole plant organ; t – treatment durations in days (d), and subscripts 1 and 2 – initial and final harvest. The TF of metals in plants was calculated by dividing the metal content in leaves by the metal content in roots.[25]

3. Results and discussion

3.1. Characteristics of ENPs in HGL medium

The ζ potential of sulph-nZnO was marginally higher at −8.8 mV compared to nano-ZnO, which measured −10.8 mV in HGL solution (ESI,† Table S5). The average aggregate size of nZnO was 350 nm, and their ζ potential may facilitate the aggregation of particles. No result of aggregate size was measured for sulph-nZnO (outside the detection limit of the instrument), because they are closer to zero ζ potential, which probably caused higher aggregation, resulting in their rapid settlement. It has to be noted that there are no significant changes in pH (6.5–6.7) compared to the control (−) (6.3). As depicted in Fig. 2, the Zn^{2+} concentrations in HGL solutions with added nZnO or sulph-nZnO remained consistent over 168 hours, ranging from 0.34 to 0.39 mg L^{-1}, which represents approximately 75% of the stock concentration of applied ENPs. This finding contrasts with

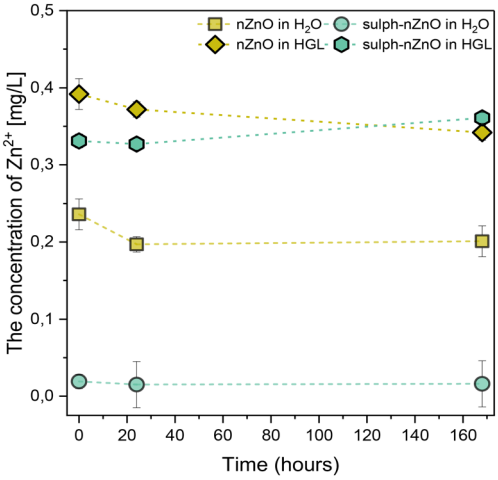

Fig. 2 The concentration of Zn^{2+} in MQ water and Hoagland medium (HGL) with nZnO and sulph-nZnO at a rate of 0.05 Zn per L measured after 0, 1, and 7 days. The concentration of Zn^{2+} was determined by the ICP-OES instrument in the previous filtered solutions using Microsep Advance centrifugal devices with omega membrane 1 K. Error bars represent standard error (n = 3 repeats).

other studies where the dissolution of sulphidized ENPs was lower than that of pristine ENPs in the growth media. For example, Ag ENPs released approximately ten times more Ag^+ than AgS ENPs in 1/2 Hunter's medium[13] and 1/2 Hoagland solution.[26] Notably, a 10-fold lower dissolution of sulph-nZnO (0.02 mg L^{-1}) compared to nZnO was observed in Milli-Q® water. This discrepancy in Zn^{2+} release from ENPs in different solutions may be attributed to the higher ionic strength in the HGL medium, which enhances ENP dissolution.[27] Furthermore, complexation of Zn^{2+} by anions such as phosphate or carbonate present in the HGL medium may also contribute to the lower concentration of free Zn^{2+}.[28,29]

3.2. Characterization of plant growth medium

The plant growth medium (after removal of the plant) was analyzed in terms of Zn^{2+} levels (Fig. 3A). In the control (−) solution, no Zn^{2+} was detected (below the limit of detection of 1 ppb), while the highest Zn^{2+} concentration (0.29 mg L^{-1}) was observed in the control (+) solution after 1 day of plant growth (Fig. 3A). The Zn^{2+} concentration in the treated solutions ranged from 0.03–0.05 to 0.17 mg L^{-1}, following this order: nZnO ≈ sulph-nZnO < $ZnSO_4$. Considering the Zn^{2+} levels measured in the pure HGL medium (without plant growing), the loss of Zn^{2+} from the solution was similar (0.29–0.35 mg of Zn^{2+}) across both ENPs and $ZnSO_4$ treatments, suggesting significant Zn^{2+} uptake by the plant or adherence of ENPs to the plant roots. After 7 days, the Zn^{2+} concentration in all the Zn compound-amended solutions stabilized at a similar level (0.01–0.04 mg L^{-1}), which was significantly lower than the control (+) solution containing 0.21 mg L^{-1}. These findings highlight differences in Zn management between Zn-deficient plants

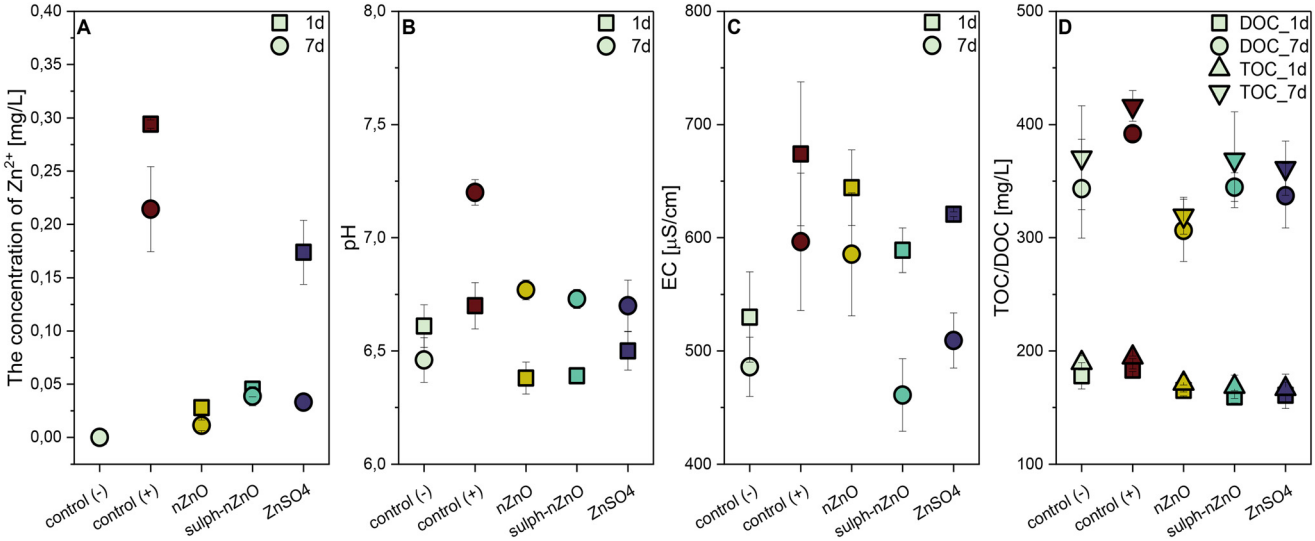

Fig. 3 Zn^{2+} concentrations (A), pH (B), EC (C), and DOC and TOC (D) in the growth medium of barley following exposure to Zn compounds for 1 and 7 days. The control (−) and the control (+) mean the untreated plants grown in HGL solutions without or with Zn ions (as $ZnSO_4$), respectively. Error bars represent standard error (n = 3 repeats).

after Zn supply ($ZnSO_4$) and Zn-sufficient plants (control (+)). Zn-deficient plants exhibited near-complete absorption of the resupplied Zn^{2+} from $ZnSO_4$, whereas Zn-sufficient plants maintained a stable Zn^{2+} concentration in the surrounding solution. This phenomenon may be attributed to nutritional memory, wherein prior deficiency conditions prime the plants for accelerated or more efficient uptake upon subsequent nutrient availability.[30] Furthermore, plants experiencing Zn deficiency may release chelating agents.[20] These agents can bind metal ions, forming larger Zn^{2+}–ligand complexes that are unable to pass through a 1 kDa filter. This complex formation could explain the observed low concentration of Zn^{2+} in the solution following the resupply of $ZnSO_4$. In the case of ENPs, the actual Zn^{2+} concentration in the plant growth medium resulted from ENP dissolution, Zn^{2+}/ENP uptake, and potential biotransformation by the plants. Thus, these results will be more informative together with the determined Zn content in plants described in the following section.

The parameters of the plant growth medium, such as pH, EC, DOC, and TOC, were also analyzed to characterize the plant-related environment (Fig. 3B–D). Given the relatively low dose of Zn and short exposure duration, the most notable differences in these parameters were observed between the control (−) and control (+). This disparity may be attributed to the varying metal acquisition strategies utilized by plants in nutrient-deficient environments, including the regulation of acidification or the secretion of root exudates to enhance nutrient bioavailability.[31] Upon exposure to Zn compounds, the changes in EC and DOC/TOC were observed in the HGL solution (Fig. 3C and D). The pH remained consistent across treatments with Zn compounds, staying within 6.4 to 6.7 over 7 days (Fig. 3B). After 7 days, the EC of solutions with nZnO or $ZnSO_4$ was about 20% higher than that of sulph-nZnO (481 µS cm^{-1}). This difference might suggest that plants absorb nutrients at different rates or that their roots release different types of metabolites.[32] Changes in the elemental composition of plants, discussed later, may further support this observation. Another critical aspect of the plant growth medium affecting ENP behavior and interactions with plants is the DOC and TOC, which relate to the secretion of plant metabolites. Root exudates and DOC have been found to expedite metal ion release from ENPs.[33,34,36] In this study, the DOC level decreased by 7–10% when exposed to Zn compounds compared to the control (−) after 1 day. The interactions between DOC and ENPs may be mutual; a study by Liu *et al.*[35] demonstrated that both pristine and sulphidized ZnO ENPs increased DOC in the maize rhizosphere, with a more significant increase than Zn^{2+} exposure alone. On the other hand, ENPs might adhere to root surfaces, potentially obstructing biomolecule exchange by clogging cell pores.[23,24] However, SEM analysis did not detect ENPs on the roots (Fig. S2†). The decrease in DOC and TOC could be associated with the determined root mass. DOC or TOC to the dry weight of roots conversion (DOC/DW_{roots}. TOC/DW_{roots}, respectively) may better reflect the plant's response to solutions enriched with Zn and both controls (Table S6†). DOC/DW_{roots} and TOC/DW_{roots} ratios follow this order: the control (+) < $ZnSO_4$ < sulph-nZnO ≈ nZnO < the control (−) (Table S6†). Zn-deficient plants tend to produce more exudates (and more DOC and TOC) to mobilize nutrients compared to those growing under optimal conditions.[20] Thus, the determined lower ratios in the plant media treated with Zn compounds compared to the control (+) might indicate Zn recovery in plants previously growing at Zn shortage.

3.3. Analysis of plant response to nanoparticulate and ionic Zn compounds

3.3.1. Plant growth. The application of Zn compounds increased the dry weight of barley tissues only after 7 days, thereby enhancing biomass (Fig. 4). However, it is noteworthy that the increase in root mass induced by ENPs was less than that observed in the control (+). Interestingly, a different pattern emerged for the dry weight of the above-ground parts, as follows: the control (−) ≈ sulph-nZnO < the control (+) ≈ nZnO < $ZnSO_4$ (Fig. 4A). The tissue-specific enhancement observed with ENPs and $ZnSO_4$ may result from distinct mechanisms governing the behavior of nanoparticulate and ionic Zn *in planta*. Specifically, the uptake and transport of targeted metal loading, as well as the regulation of other elemental interactions may have a different course for Zn particles and ions.[17] Furthermore, due to the relatively brief exposure period, the treatment's impact on overall biomass may be delayed. Another indicator of plant growth, the relative growth rate, demonstrated that the addition of Zn compounds accelerated the growth of barley (Fig. 4B) compared to both controls. These results confirm that, irrespective of the form in which Zn was applied, all treatments consistently enhanced plant growth, in line with Zn's recognized role as an essential micronutrient.

3.3.2. Zn loading to plants. The treatment of plants with nanoparticulate and ionic Zn experiencing Zn deficiency resulted in an increased Zn content within the tissues (Fig. 5A). A significant portion of Zn accumulated in the aboveground parts of plants, likely due to the critical demand for Zn during the tillering stage, which is a period of intense growth.[37] After 1 day, the Zn content in shoots was the highest with sulph-nZnO and $ZnSO_4$ treatments (26 mg kg^{-1}), followed by nZnO (19.4 mg kg^{-1}). Furthermore, all Zn treatments led to higher Zn acquisition compared to both the control (+) (15.7 mg kg^{-1}) and the control (−) (2.6 mg kg^{-1}). The elevated Zn levels in the shoots of treated plants, compared to the Zn-sufficient plants (control (+)), confirmed the more intensive Zn acquisition in deficient plants. Additionally, as indicated by the translocation factors (Fig. 5A), there was stronger root-to-shoot translocation in treated plants compared to the control (+), supporting the above assumption. This response is likely attributable to the plants' stress memory resulting from prior Zn deficiency.[38] The Zn distribution pattern in roots differed from that in shoots (Fig. 5A). All Zn treatments resulted in lower Zn levels in roots than in the control (+), yet higher than the control (−). Sulph-nZnO increased Zn loading in roots by 42% compared to nZnO (7.1 mg kg^{-1}), while no significant difference was noted between nanoparticulate and ionic Zn in roots.

The distribution of Zn in barley changed over time (Fig. 5A). There was no difference in Zn content in roots between ENPs (12.4–14.8 mg kg^{-1}), but $ZnSO_4$ led to a 15% to 28% higher Zn content, similar to the control (+). Meanwhile the Zn shoot level was as follows: the control (−) < the control (+) < nZnO < sulph-nZnO < $ZnSO_4$. Interestingly, despite a similar dissolution rate in the fresh medium and loss of Zn^{2+} in the growth medium, Zn accumulation in plants was higher when exposed to sulph-nZnO than nZnO. This contrasts with other studies on sulphidized metal-based ENPs, which often show reduced accumulation of target metal from sulph-nENPs compared to pristine ENPs due to decreased dissolution.[15,39] A study by Wang *et al.*[39] demonstrated a twofold lower accumulation of Ag in wheat shoots exposed to Ag_2S ENPs for two weeks compared to Ag ENPs, despite a tenfold higher applied dose of Ag_2S ENPs. However, sulph-nZnO, in addition to Zn^{2+}, could also be a

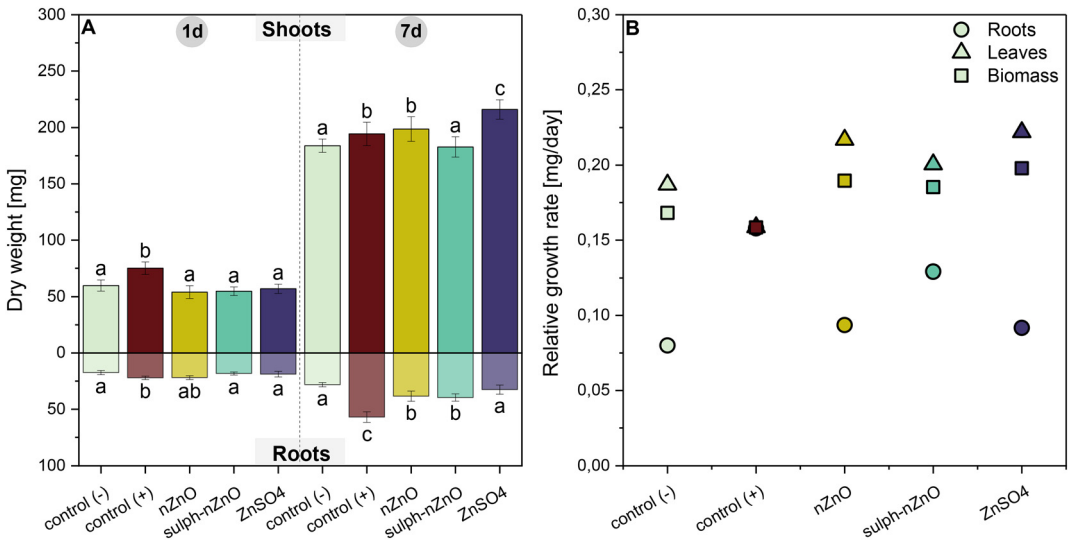

Fig. 4 The dry weight of barley roots and shoots (A) and relative growth rate of plants (B) exposed to Zn compounds at 0.5 mg Zn L^{-1}. Error bars represent standard error (n = 3 biological repeats). The control (−) and the control (+) mean the untreated plants grown in HGL solutions without or with Zn ions (as $ZnSO_4$), respectively. Different letters indicate significant differences among the treatments (Tukey test, $p < 0.05$).

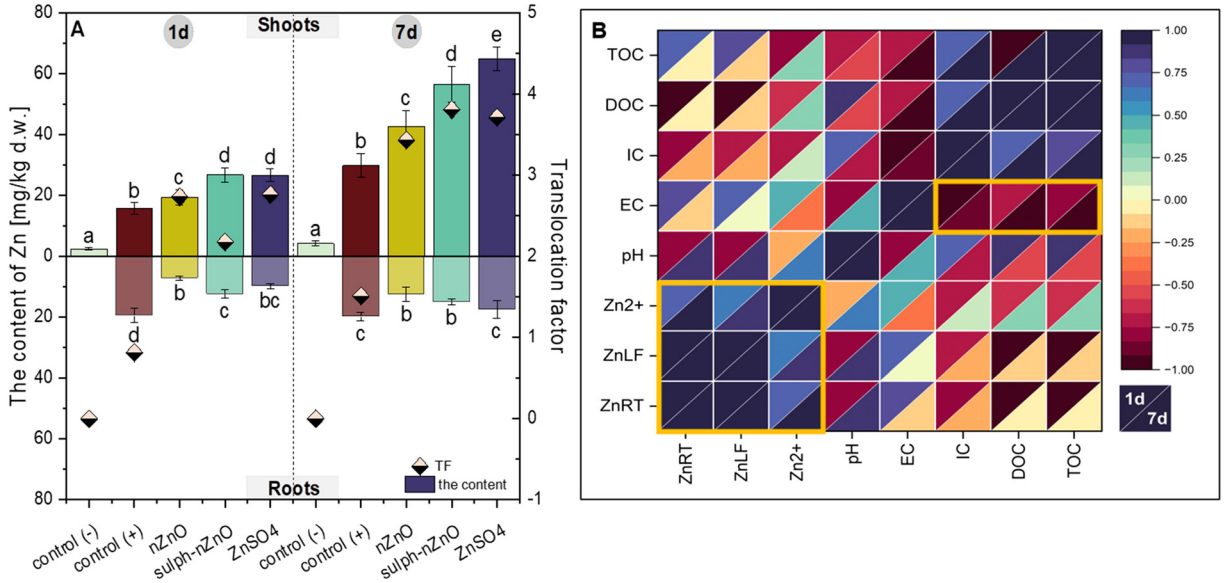

Fig. 5 The content and translocation factor of Zn (A) in *H. vulgare* exposed to nZnO, sulph-nZnO and $ZnSO_4$ (at 0.05 mg Zn L^{-1}) for 1 and 7 days. The control (–) and the control (+) mean the untreated plants grown in HGL solutions without or with Zn ions (as $ZnSO_4$), respectively. Erro bars represent standard error (n = 3 biological repeats). Different letters indicate significant differences among the treatments (Tukey test, $p < 0.05$). The correlation plot (B) between the Zn content in plant tissues and parameters of growth medium.

source of S, which is crucial for synthesizing key amino acids and proteins.[40] The delivery of S^- or SO_4^{2-} would enhance S-related biosynthetic pathways, including the production of glutathione, which is one of the most important metal chelators and antioxidants.[41] An increase in endogenous and extraneous glutathione content has improved Zn transport from roots to leaves in *Brassica rapa*[42] and *Arabidopsis thaliana*[43] under non-excessive Zn conditions. Therefore, the glutathione-related pathway could be responsible for the higher loading of sulph-nZnO ENPs in Zn-deficient barley during intense growth. Moreover, sulph-nZnO is characterized by a smaller particle size than pristine nZnO, which may favor their uptake and transport in plants.[44] The absorption of solid particles *via* roots is size-limited. For instance, Milewska-Hendel *et al.*[45] measured the pore size of the cell wall of the barley rhizodermis to be between 2.2 nm and 7.2 nm. Sulph-ZnO, characterized by a less negative zeta potential, may facilitate its uptake in comparison to nano-ZnO, which is likely to experience stronger repulsion from negatively charged roots. However, both ENPs exhibited lower Zn loading than $ZnSO_4$, indicating that metal ions are more readily absorbed, as reported in previous studies.[46] It should

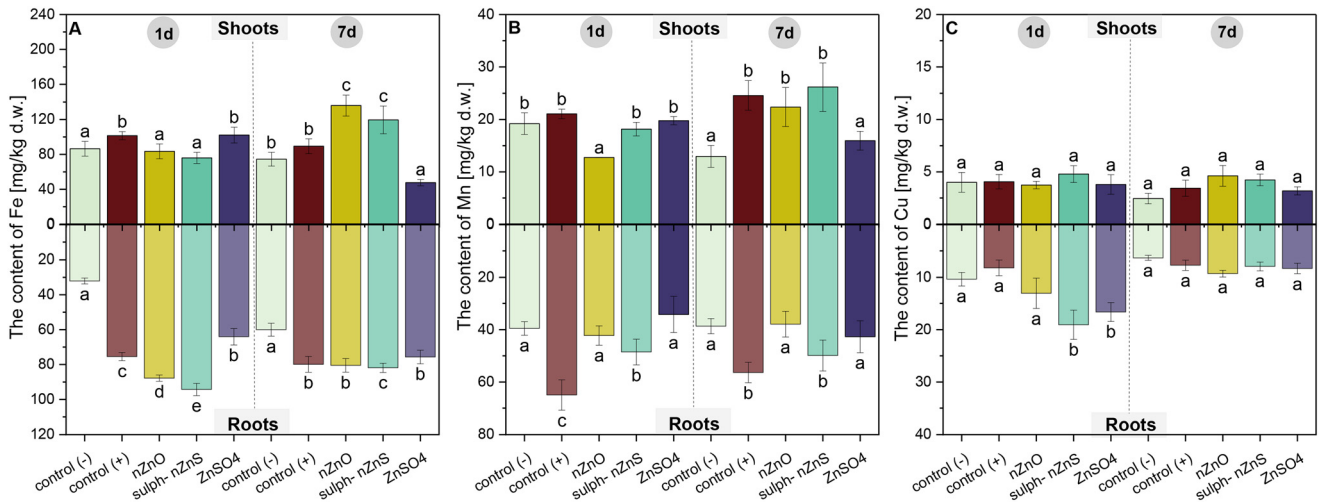

Fig. 6 The content of Fe (A), Mn (B), and Cu (C) in barley shoots and roots treated with ENPs (nZnO, sulph-nZnO) or metal salts (at 0.5 mg Zn L^{-1}) after 1 and 7 days of exposure. The control (–) and the control (+) mean the untreated plants grown in HGL solutions without or with Zn ions (as $ZnSO_4$), respectively. Error bars represent standard error (n = 3 biological repeats). Different letters indicate significant differences among the treatments (Dunnett's test, $p < 0.05$).

be noted that the correlation plot (Fig. 5B) displayed no significant relation between Zn content and the parameters of the medium (pH, EC, IC, DOC, TOC, Zn^{2+}), which may indicate that the properties other than Zn ions/particles impact Zn accumulation in these plants.

3.3.3. Other transition metals' content. Due to the strong cross-talk between Zn and other transition metals *in planta*,[21] which results in differing compositions between Zn-deficient and Zn-sufficient plants, it is necessary to assess the impact of Zn compound treatments on the accumulation of other elements. Our study demonstrated fluctuations in the levels of Fe, Mn, and Cu in plants exposed to various Zn compounds (Fig. 6). At the onset of exposure (1 day), the contents of Fe, Mn, and Cu were primarily altered in the barley roots, which were in direct contact with the Zn compounds. Sulph-nZnO, followed by nZnO, induced a significant 1.7–1.9-fold increase in Fe content in the roots (respectively, 94.3 and 87.3 mg per kg d.w.), surpassing even the levels in the control (+), whereas the Fe increase induced by $ZnSO_4$ (64.1 mg per kg d.w.) was lower but still significantly higher than the control (−) (Fig. 6A). The increased Fe content might compensate for the low Zn levels, as the supplied Zn is rapidly translocated to the shoots.[47] However, it is puzzling that the Fe levels did not align with

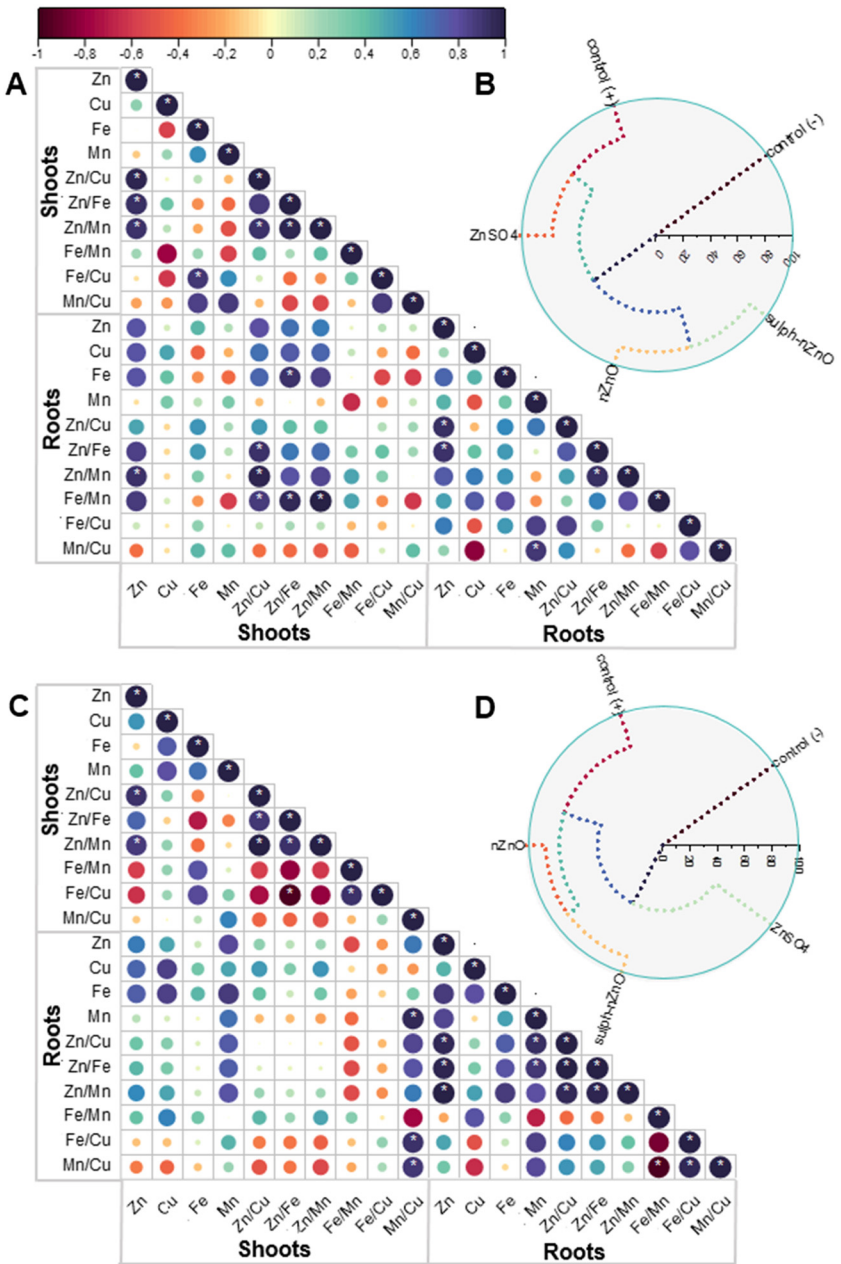

Fig. 7 The correlation plot (A and C) and cluster plot (B and D) performed for transition metal contents or ratios in barley observed after 1 (A and B) and 7 days (C and D). Statistically significant Pearson correlation factors ($p < 0.05$) are marked with an asterisk.

Zn content in the treated roots. Moreover, Mn levels were affected only by sulph-nZnO, which increased its content by 22% compared to the control (−) (Fig. 6B), while Cu accumulation in roots was enhanced by sulph-nZnO and $ZnSO_4$ by 60–83% relative to both controls (Fig. 6C). In the shoots, single variations in Fe and Mn content were observed under Zn exposure: $ZnSO_4$ raised Fe concentrations to levels noted in the control (+), whereas nZnO reduced Mn levels by 33% compared to both controls. After 7 days, the Fe and Cu content in roots showed less variability among Zn-treated samples and were similar to Zn-sufficient plants (Fig. 6A and C). Conversely, the Mn root pattern remained unchanged after 7 days (Fig. 6B). A significant difference in Fe and Mn content in shoots was observed between nanoparticulate and ionic Zn: both ENPs increased Fe levels by 60.4–82.4% (exceeding the control (+) as well), while $ZnSO_4$ decreased Fe levels by 63% compared to the control (−). nZnO and sulph-nZnO caused a 72.7% and 101.9% increase in Mn levels, respectively, while $ZnSO_4$ did not differ from the control (−). The Cu levels in shoots remained unchanged.

The observed changes in transition metal contents under Zn treatments in roots and shoots confirm a complex interplay between these elements, despite the absence of a significant correlation between transition metal concentrations in barley tissues (Fig. 7). Variations in the microelement level may result from their competition for transceptors and sensors.[47] According to the Irving–Williams series, the relative binding affinities of divalent metals for ligands, such as nicotianamine, phytosiderophores (*e.g.*, mugineic acid), organic acids (*e.g.*, citrate, malate), and amino acids (*e.g.*, histidine),[48] are Mn < Fe < Zn < Cu.[49] Additionally, the plants may perceive the concentration ratios between transition metals rather than the individual metal contents.[50] Our study identified some correlations between metal contents and metal ratios, particularly during the first day of exposure when Zn transport is intense (Fig. 7). Most of these correlations involved two metals, though some connections extended to different metals *e.g.* Mn content in roots was positively correlated with the Zn/Mn ratio after 7 days (Fig. 7C). It implies the cross-metal nature of metal composition and highlights the complex machinery of metal acquisition.[51]

Furthermore, the cluster analysis revealed significant differences in the elemental composition patterns of plants exposed to nanoparticulate and ionic Zn (Fig. 7B and D). This may be attributed to the different interaction dynamics between ENPs and roots, including adsorption and root mucilage composition, compared to Zn ions. Liu *et al.*[35] observed a different profile of metabolites by roots exposed to sulphidized ZnO ENPs (including amino acids such as histidine and cysteine) compared to pristine ones, which may influence nutrient foraging among Zn treatments. Many studies on the effect of pristine ENPs on hydroponically or soil-grown plants have reported different plant elemental composition patterns from those of their ionic counterparts.[17,46,52,53] These differences arise from the distinct transport mechanisms of ENPs, which are processed as solid particles, compared to ionic metals.[54] A decrease in Fe levels in leaves was observed in soil-grown barley exposed to $ZnSO_4$ for 30 days, while the exposure to nZnO did not affect Fe content.[46] A similar trend was noted in *A. thaliana* seedlings, despite differing metal acquisition strategies between monocots and dicots.[21] Little is known about the effects of sulphidized ENPs on plant elemental composition. Few studies have shown the potential of foliar-applied synthesized ZnS to enhance the nutritional value of mungbean[55] or soil-grown plants, but without comparisons to metal oxides or salts.[56] The highest increase in transition metal content in roots by sulph-nZnO may be linked to the supplementary supply of S alongside Zn. It has been demonstrated that S supports Fe uptake by plants, including cereals, through increased release of phytosiderophores by roots to accelerate Fe uptake.[57] The phytosiderophores may also acquire other trace metals.[58] It is important to note that, after 7 days, the accumulation pattern of Zn, Cu, Mn, and Fe for ENPs was the closest to the composition of Zn-sufficient plants (the control (+)) and more distinct from $ZnSO_4$, contrary to the 1 day exposure. This suggests that the modulation of chemically similar micronutrients by ENPs was more sustainable compared to Zn ions. The most significant differentiation between ionic and nanoparticulate Zn was their opposite effects on Fe and Mn levels. The exposure to $ZnSO_4$ decreased shoot Fe and Mn, while both ENPs increased their levels. The reduction in Fe and Mn concentrations has been reported as a consequence of excess Zn in various plants exposed to relatively high concentrations.[57] It may suggest that $ZnSO_4$ treatment causes an overload of Zn in tissues, resulting in a decrease of other transition metals in the plant

3.3.4. Macroelement concentration. The content of K, Ca, and Mg in the plant was also significantly altered under Zn exposure (Fig. 8). However, the pattern of changes differed depending on the form of Zn applied, the plant tissue, and the duration of exposure. The K level changed only under exposure to ENPs for 1 day, with K content decreasing by 15–22% in both roots and shoots compared to the control (−), similar to plants grown under Zn-sufficient conditions (Fig. 8A). After 7 days, K accumulation varied only in shoots across samples as follows: control (−) < control (+) ≈ $ZnSO_4$ < nZnO ≈ sulph-nZnO. The observed increase in K content in Zn-treated plants may reflect changes in root membrane permeability and/or modifications in root architecture, such as fine root or root hair proliferation, which can enhance K^+ uptake.[20,59] Under Zn-deficient conditions, a decrease in suberin accumulation in roots, possibly linked to altered ROS homeostasis, can increase membrane permeability and contribute to K^+ leakage.[19] Consequently, as Zn is absorbed and loaded into the plant, it may enhance the impermeability of roots, thereby reducing the loss of K^+. The higher root hair density under Zn-deficiency conditions may also enhance K acquisition.[59] In truth, K content did not correspond to Zn

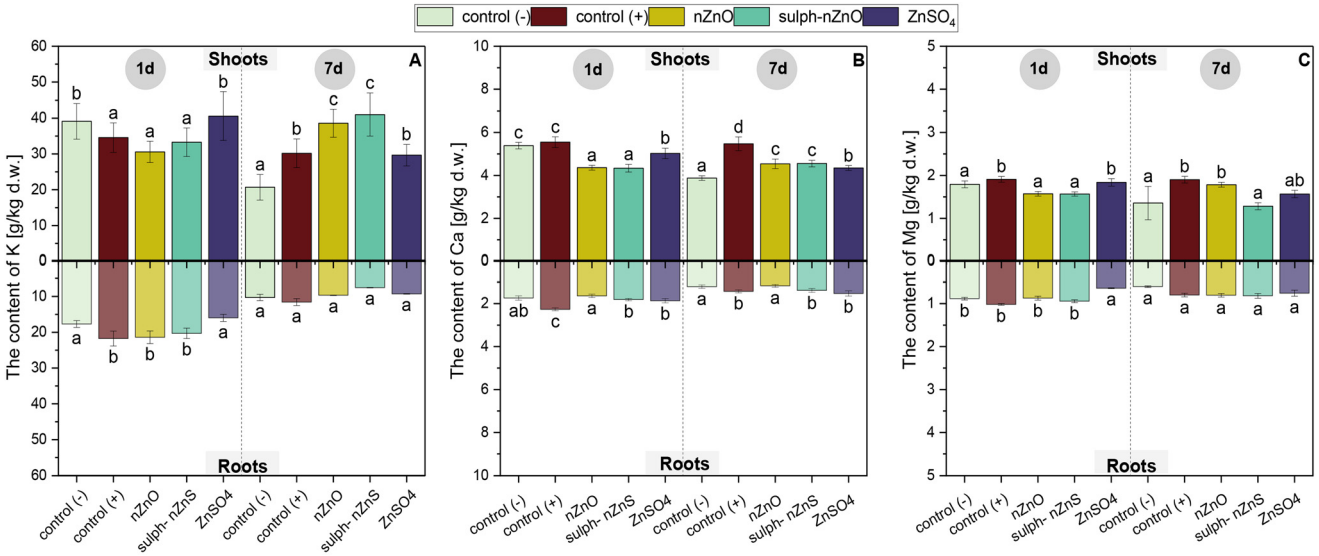

Fig. 8 The content of K (A), Ca (B), and Mg (C) in barley shoots and roots treated with ENPs (nZnO, sulph-nZnO) or metal salts (at 0.5 mg_{Zn} L^{-1}) after 1 and 7 days of exposure. The control (–) and the control (+) mean the untreated plants grown in HGL solutions without or with Zn ions (as $ZnSO_4$), respectively. Error bars represent standard error (n = 3 biological repeats). Different letters indicate significant differences among the treatments (Dunnett's test, $p < 0.05$).

accumulation levels under ENPs and $ZnSO_4$ exposure, but a close relation between the translocation factors of Zn and K was found after 7 days (Fig. S3†).

Ca content in roots was unaffected after 1 day of exposure to Zn compounds compared to the control (–) and was 17.5–27.5% lower compared to the control (+) (Fig. 8B). The Ca level in shoots of treated plants decreased by 7–20% compared to both controls. After 7 days of exposure to Zn compounds, Ca content in roots aligned with that in untreated plants. In contrast, Ca accumulation in shoots

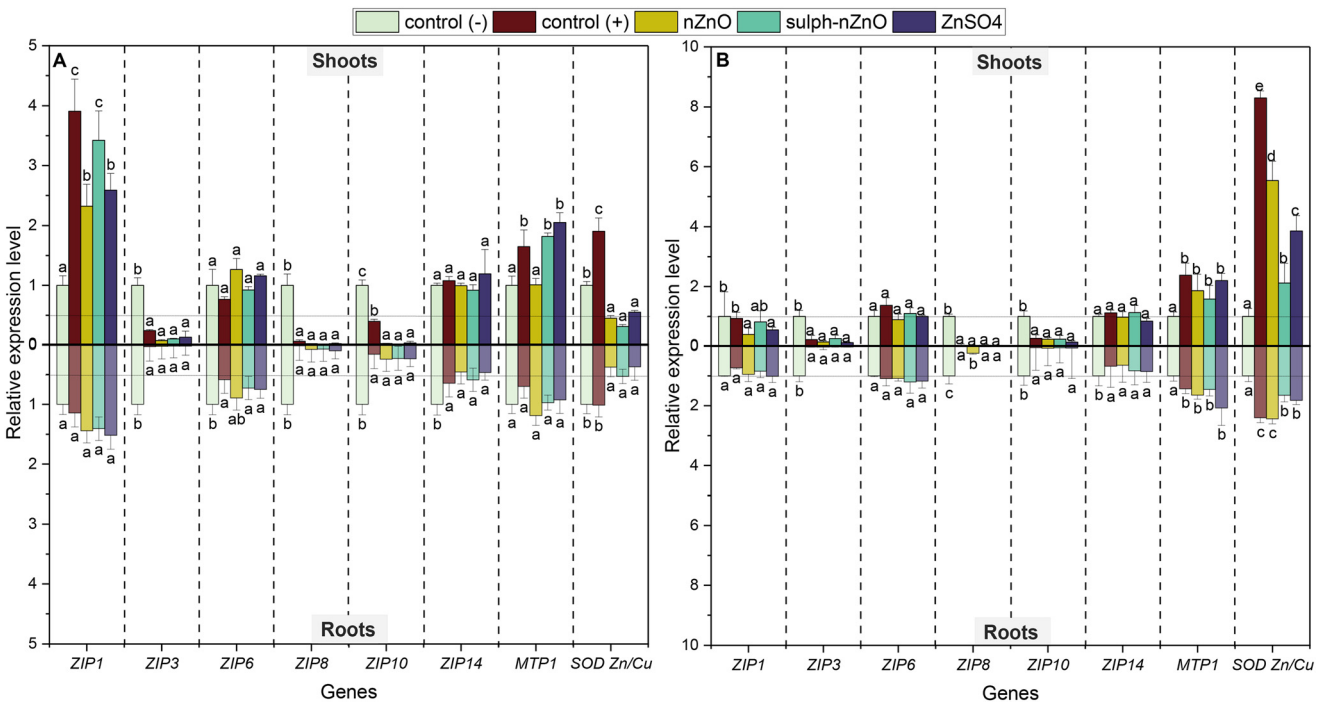

Fig. 9 The relative expression of genes related to Zn homeostasis in barley roots and shoots exposed for 1 (A) and 7 days (B) to nZnO, sulph-nZnO, and $ZnSO_4$. The control (–) and the control (+) mean the untreated plants grown in HGL solutions without or with Zn ions (as $ZnSO_4$), respectively. Error bars represent standard error (n = 3 biological repeats). Different letters indicate significant differences among the treatments (Tukey test, $p < 0.05$).

increased by 12–17% under Zn treatments compared to the control (−) but remained 17–20% lower than in the control (+). After 1 day, Mg levels in roots changed only with exposure to $ZnSO_4$, which reduced its content by 27% compared to the control (−) (Fig. 8C). Over time, Mg accumulation in roots became similar in treated and untreated samples. In shoots, Mg levels were as follows: control (−) ≈ sulph-nZnO < $ZnSO_4$ < nZnO ≈ control (+). Considering that the decline of Mg and Ca (divalent cations) was mostly observed under Zn treatments, it may be attributed to both specific competition for shared transporters and non-specific electrostatic interference by elevated Zn^{2+} levels, which hinder the uptake or translocation of other essential divalent ions due to overlapping affinity or electrochemical gradients.[47]

3.3.5. Gene expression pattern. To accurately assess metal acquisition, it is essential to consider additional markers of cellular metal status apart from elemental composition. Consequently, our study also analyzed gene expression associated with metal homeostasis (Fig. 9). Multiple members of the ZIP family are known to mediate both the uptake and root-to-shoot translocation of Zn in cereals,[60–62] including barley.[63] In our study, three genes from the ZIP family (*ZIP3, ZIP8, ZIP10*) were identified as Zn deficiency-inducible genes due to their significantly higher transcript levels in Zn-deficient compared to Zn-sufficient barley (Fig. 9). This trend was observed in both roots and shoots, confirming the involvement of these transporters in the absorption and transport of Zn from roots to above-ground parts.[63] In contrast, tissue-specific expression was observed in Zn-deficient plants for *ZIP1*, *ZIP6*, and *ZIP14*. Zn deficiency led to increased transcripts of *ZIP6* and *ZIP14* only in roots compared to Zn-sufficient conditions, reflecting the enhanced capacity of Zn scavenging by roots during Zn deprivation.[63] Treatment with Zn compounds resulted in the down-regulation of genes involved in uptake (*ZIP6*, *ZIP14*) and root-shoot translocation (*ZIP3, ZIP8, ZIP10*) to levels similar to the control (+). This indicates a rapid recovery of Zn balance under treatment, regardless of the Zn form used. Notably, Zn-treated plants had comparable amounts of Zn in roots or shoots among treatments, similar to the regular content measured in Zn-efficient plants (approximately 20 mg per kg dry weight).[64] A similar response (down-regulation) of Zn deficiency-inducible genes to ZnO ENPs and Zn^{2+} was observed in the roots of hydroponically grown *A. thaliana*[18] and the shoots and roots of soil-grown *A. thaliana.*[17] Interestingly, differences among Zn treatments were observed in the expression of *ZIP1* in shoots, where the transcript level for sulph-nZnO was as high as in Zn-sufficient plants and 1.5-fold higher than the up-regulation induced by nZnO and $ZnSO_4$ (Fig. 9A). Although *ZIP1* is a Zn-responsive gene, it plays a role in Zn efficiency,[63] as it was up-regulated in the shoots of Zn-sufficient plants compared to Zn-deficient conditions. Specifically, *ZIP1* may be associated with the efflux of Zn from the cytoplasm into intercellular spaces, indicating a slightly redundant Zn pool. Our analysis showed

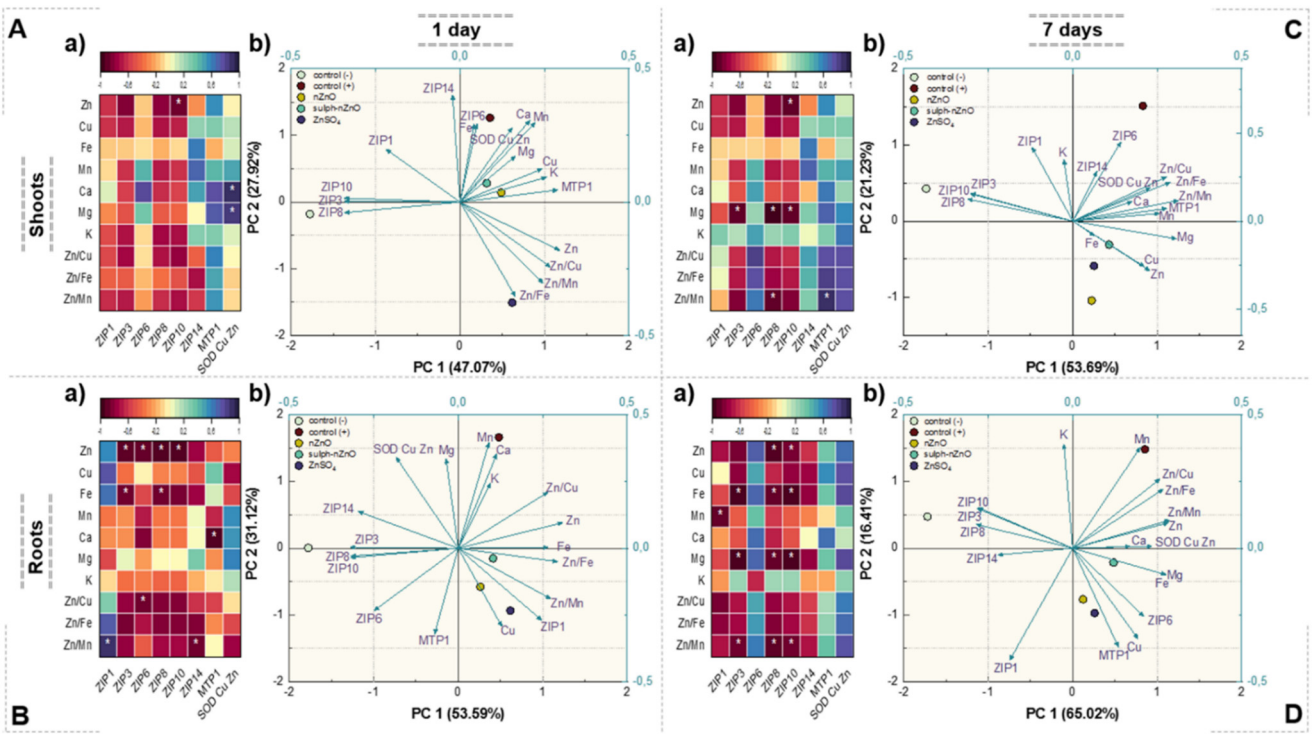

Fig. 10 The correlation plot (a) and PCA plot consisting of loadings and scores (b) performed for the transcript of genes and the elemental composition determined in the shoots and roots of barley after 1 (A and B) and 7 days (C and D). Statistically significant Pearson correlation factors ($p < 0.05$) are marked with an asterisk.

similar Zn levels in shoots for sulph-nZnO and $ZnSO_4$, which were higher than for nZnO, but this did not overlap with the observed *ZIP1* transcript pattern. Although the ZIP family consists of Zn-responsive genes, evidence suggests that *ZIP1* is also affected by the levels of other elements or their ratios.[21] The correlation and PCA plots revealed no correlation between the transcript level of *ZIP1* and Zn level, but there was a relationship between *ZIP1* expression and the ratios of transition metals (Fig. 10). Furthermore, even though ionic and nanoparticulate Zn induce a similar pattern of gene expression, the mechanisms of action could differ.[22] For instance, solid particles attached to cells might also upregulate metal transporters.

Interestingly, the expression of *MTP1* differed under Zn treatment in shoots after 1 day of exposure (Fig. 9). MTP1 is a transporter localized in the tonoplast, recognized for facilitating Zn^{2+} efflux from the cytoplasm into the vacuole to regulate cellular Zn levels.[64] The up-regulation of *MTP1* could suggest Zn saturation in the shoots due to the highest Zn loading under sulph-nZnO and $ZnSO_4$. Despite nZnO also increasing the Zn shoot, no change in *MTP1* transcript was noted that the Zn content may include nanoparticulate and ionic Zn, which may evoke a distinct transcriptional response. In turn, *Cu/ZnSOD*, encoding the Zn-requiring enzyme, in treated plants (in both roots and shoots), was down-regulated compared to Zn-deficient and Zn-sufficient plants (Fig. 8A). Cu/ZnSOD is a metalloenzyme that scavenges peroxides, a type of reactive oxygen species.[65] The abundance of *Cu/ZnSOD* transcript is related to Zn availability, and its expression is up-regulated in Zn-sufficient plants compared to Zn-deficient conditions, as observed in our study. The decrease in *Cu/ZnSOD* transcripts in barley tissues was noted regardless of the Zn form applied, despite significant Zn acquisition. This could suggest that the delivered Zn was allocated to more urgent demands, especially since Cu/ZnSOD could be compensated for by other SOD isoforms (MnSOD, FeSOD) in cases of Zn and Cu deprivation.[66] In addition, the content of Fe and Mn positively correlated with *Cu/ZnSOD* transcripts, particularly in shoots Fig. 10Ab).

Changes in gene expression over time were observed only for three genes (*ZIP1, MTP1, Cu/ZnSOD*) (Fig. 9B). Unlike the first day of exposure, no differences in transcripts of *ZIP1* and *MTP1* were observed among Zn treatments in barley after 7 days. The down-regulation of *ZIP1* and the up-regulation of *MTP1* may aim to retain Zn in cells and accumulate Zn in the vacuole due to subsequent Zn loading. After 7 days, *Cu/ZnSOD* transcripts in treated plants were higher than in Zn-deficient plants, indicating the restoration of Cu/ZnSOD function. However, a score plot shows that Cu/ZnSOD transcript levels were more related to the Zn/Cu ratio than the Zn level (Fig. 10Ca and b). Among treatments, the up-regulation of *Cu/ZnSOD* was twice as high under nZnO exposure, similar to Zn-sufficient plants, compared to sulph-nZnO. ENPs are known to modulate the plant defense system in response to oxidative stress.[18,67,68] Zn deficiency results in the oxidative stress in plants, and the up-regulation of the *Cu/ZnSOD* gene could indicate the recovery of the SOD enzyme and the activity of the defense system as well. This response might also result from the generation of ROS by ENPs and metal ions, which was observed for ZnO ENPs in the previous studies.[25,69]

4. Conclusions

The integrative chemical and transcriptional analysis presented the initial recovery of Zn in Zn-deficient plants using sulphidized ZnO ENPs compared to pristine ZnO ENPs and metal ions. The sulphidized ZnO nanoparticles demonstrated superior Zn uptake and acquisition of some other metals than the pristine ENPs, despite similar Zn^{2+} release in the plant growth medium. Although $ZnSO_4$ resulted in the highest Zn delivery to Zn-deficient plants, certain characteristics suggest potential overloading, as indicated by decreased transition metal content. However, the pattern of molecular markers did not considerably differ between Zn treatments. Considering that statistical analysis shows distinctly different patterns of chemical traits induced by ENPs from metal ions, ENPs may be a promising alternative to traditional agents for the enhancement of the nutritional quality of plants.

Data availability

Data for this article are available at **https://doi.org/10.5281/zenodo.14329331**.

Conflicts of interest

There are no conflicts to declare.

Acknowledgements

We are grateful to Magdalena Kusiak Ph.D., for her support in the real-time qPCR analysis. This study was funded by the National Science Centre (Poland) in the frame of the OPUS project (2021/43/B/NZ9/02857).

References

1 C. Stanton, D. Sanders, U. Krämer and D. Podar, *Mol. Plant*, 2022, **15**, 65–85.
2 *Micronutrient deficiencies in global crop production*, ed. B. J. Alloway, Springer, Dordrecht, 2008.
3 M. Kusiak, P. Oleszczuk and I. Jośko, *J. Hazard. Mater.*, 2022, **424**, 127374.
4 M. Kah, R. S. Kookana, A. Gogos and T. D. Bucheli, *Nat. Nanotechnol.*, 2018, **13**, 677–684.
5 M. Kah, N. Tufenkji and J. C. White, *Nat. Nanotechnol.*, 2019, **14**, 532–540.
6 European Commission, Communication From The Commission To The European Parliament, The Council, The European Economic And Social Committee And The Committee Of The Regions, *Farm to Fork Strategy*, 2020, COM(2020)381.

7 H. Sturikova, O. Krystofova, D. Huska and V. Adam, *J. Hazard. Mater.*, 2018, **349**, 101–110.
8 G. V. Lowry, K. B. Gregory, S. C. Apte and J. R. Lead, *Environ. Sci. Technol.*, 2012, **46**, 6893–6899.
9 I. Jośko, P. Oleszczuk, J. Dobrzyńska, B. Futa, J. Joniec and R. Dobrowolski, *Geoderma*, 2019, **352**, 204–212.
10 I. Jośko, M. Kusiak and P. Oleszczuk, *Chemosphere*, 2021, **266**, 128982.
11 P. Oleszczuk, B. Czech, M. Kończak, A. Bogusz, A. Siatecka, P. Godlewska and M. Wiesner, *Chemosphere*, 2019, **237**, 124359.
12 C. Levard, B. C. Reinsch, F. M. Michel, C. Oumahi, G. V. Lowry and G. E. Brown, *Environ. Sci. Technol.*, 2011, **45**, 5260–5266.
13 J. P. Stegemeier, B. P. Colman, F. Schwab, M. R. Wiesner and G. V. Lowry, *Environ. Sci. Technol.*, 2017, **51**, 4936–4943.
14 L. Li, L. Hu, Q. Zhou, C. Huang, Y. Wang, C. Sun and G. Jiang, *Environ. Sci. Technol.*, 2015, **49**, 2486–2495.
15 Z. Khodaparast, C. A. M. van Gestel, R. A. Verweij, A. G. Papadiamantis, S. F. Gonçalves, I. Lynch and S. Loureiro, *J. Hazard. Mater.*, 2022, **435**, 128880.
16 B. Ahmed, A. Rizvi, A. Syed, A. M. Elgorban, M. S. Khan, H. A. AL-Shwaiman, J. Musarrat and J. Lee, *J. Hazard. Mater.*, 2021, **419**, 126493.
17 P. M. G. Nair and I. M. Chung, *Sci. Total Environ.*, 2017, **575**, 187–198.
18 P. Landa, S. Prerostova, S. Petrova, V. Knirsch, R. Vankova and T. Vanek, *Environ. Sci. Technol.*, 2015, **49**, 14537–14545.
19 P. Grünhofer, L. Schreiber and T. Kreszies, in *Rhizobiology: Molecular Physiology of Plant Roots*, ed. S. Mukherjee and F. Baluška, Springer International Publishing, Cham, 2021, pp. 333–378.
20 A. Jain, B. Sinilal, G. Dhandapani, R. B. Meagher and S. V. Sahi, *Environ. Sci. Technol.*, 2013, **47**, 5327–5335.
21 S. Amini, B. Arsova and M. Hanikenne, *Plant, Cell Environ.*, 2022, **45**, 1339–1361.
22 M. Kusiak, M. Sozoniuk, C. Larue, R. Grillo, K. Kowalczyk, P. Oleszczuk and I. Jośko, *NanoImpact*, 2023, **31**, 100472.
23 T. N. M. da Cruz, S. M. Savassa, G. S. Montanha, J. K. Ishida, E. de Almeida, S. M. Tsai, J. Lavres Junior and H. W. Pereira de Carvalho, *Sci. Rep.*, 2019, **9**, 10416.
24 I. Jośko, M. Kusiak, M. Sozoniuk, M. Feculak, K. C.-W. Wu, M. Fitzgerald, M. S. Alyafei and M. S. Sheteiwy, *Sci. Total Environ.*, 2024, **918**, 170673.
25 I. Jośko, M. Kusiak, P. Oleszczuk, M. Świeca, M. Kończak and M. Sikora, *Sci. Total Environ.*, 2021, **782**, 146883.
26 J. P. Stegemeier, F. Schwab, B. P. Colman, S. M. Webb, M. Newville, A. Lanzirotti, C. Winkler, M. R. Wiesner and G. V. Lowry, *Environ. Sci. Technol.*, 2015, **49**, 8451–8460.
27 B. A. Chambers, A. R. M. N. Afrooz, S. Bae, N. Aich, L. Katz, N. B. Saleh and M. J. Kirisits, *Environ. Sci. Technol.*, 2014, **48**, 761–769.
28 S. K. Misra, A. Dybowska, D. Berhanu, S. N. Luoma and E. Valsami-Jones, *Sci. Total Environ.*, 2012, **438**, 225–232.
29 P. McManus, J. Hortin, A. J. Anderson, A. R. Jacobson, D. W. Britt, J. Stewart and J. E. McLean, *Environ. Toxicol. Chem.*, 2018, **37**, 2619–2632.
30 T. J. A. Bruce, M. C. Matthes, J. A. Napier and J. A. Pickett, *Plant Sci.*, 2007, **173**, 603–608.
31 T. Aftab and K. R. Hakeem, *Plant Micronutrients: Deficiency and Toxicity Management*, Springer Nature, 2020.
32 J. M. Moreira Barradas, B. Dida, S. Matula and F. Dolezal, *Irrig. Sci.*, 2018, **36**, 133–142.
33 H. Shang, H. Guo, C. Ma, C. Li, B. Chefetz, T. Polubesova and B. Xing, *Sci. Total Environ.*, 2019, **690**, 502–510.
34 C. Jiang, G. R. Aiken and H. Hsu-Kim, *Environ. Sci. Technol.*, 2015, **49**, 11476–11484.
35 L. Liu, O. V. Tsyusko, J. M. Unrine, S. Liu, Y. Liu, L. Guo, G. Wei and C. Chen, *Environ. Sci. Technol.*, 2023, **57**, 8943–8953.
36 F. Basit, X. He, X. Zhu, M. S. Sheteiwy, T. Minkina, S. Sushkova, I. Josko, J. Hu, W. Hu and Y. Guan, *Environ. Geochem. Health*, 2023, **45**, 4165–4179.
37 B. J. Alloway, in *Micronutrient Deficiencies in Global Crop Production*, ed. B. J. Alloway, Springer Netherlands, Dordrecht, 2008, pp. 1–39.
38 F. Gama, T. Saavedra, J. P. da Silva, M. G. Miguel, A. de Varennes, P. J. Correia and M. Pestana, *Plant Physiol. Biochem.*, 2016, **104**, 36–44.
39 P. Wang, N. W. Menzies, E. Lombi, R. Sekine, F. P. C. Blamey, M. C. Hernandez-Soriano, M. Cheng, P. Kappen, W. J. G. M. Peijnenburg, C. Tang and P. M. Kopittke, *Nanotoxicology*, 2015, **9**, 1041–1049.
40 G. Courbet, K. Gallardo, G. Vigani, S. Brunel-Muguet, J. Trouverie, C. Salon and A. Ourry, *J. Exp. Bot.*, 2019, **70**, 4183–4196.
41 Y. Wang, C. Deng, L. Zhao, C. O. Dimkpa, W. H. Elmer, B. Wang, S. Sharma, Z. Wang, O. P. Dhankher, B. Xing and J. C. White, *ACS Nano*, 2024, **18**, 11813–11827.
42 S. Nakamura, A. Wongkaew, Y. Nakai, H. Rai and N. Ohkama-Ohtsu, *Plant Sci.*, 2019, **283**, 424–434.
43 A. Wongkaew, S. Nakamura, N. Suzui, Y.-G. Yin, S. Ishii, N. Kawachi, K. Kojima, H. Sekimoto, T. Yokoyama and N. Ohkama-Ohtsu, *Plant Sci.*, 2019, **283**, 416–423.
44 Z. Lv, H. Sun, W. Du, R. Li, H. Mao and P. M. Kopittke, *Sci. Total Environ.*, 2021, **796**, 148927.
45 A. Milewska-Hendel, M. Zubko, J. Karcz, D. Stróż and E. Kurczyńska, *Sci. Rep.*, 2017, **7**, 3014.
46 I. Jośko, M. Kusiak, B. Xing and P. Oleszczuk, *J. Hazard. Mater.*, 2021, **416**, 126230.
47 X. Fan, X. Zhou, H. Chen, M. Tang and X. Xie, *Front. Plant Sci.*, 2021, **12**, 663477.
48 I. V. Seregin and A. D. Kozhevnikova, *Photosynth. Res.*, 2021, **150**, 51–96.
49 C. A. Blindauer and R. Schmid, *Metallomics*, 2010, **2**, 510–529.
50 T. Kobayashi, *Plant Cell Physiol.*, 2019, **60**, 1440–1446.
51 K. Bashir, S. Rasheed, T. Kobayashi, M. Seki and N. K. Nishizawa, *Front. Plant Sci.*, 2016, **7**, 1192.
52 C. García-Gómez, S. García, A. F. Obrador, D. González, M. Babín and M. D. Fernández, *Ecotoxicol. Environ. Saf.*, 2018, **160**, 222–230.

53 C. García-Gómez, A. Obrador, D. González, M. Babín and M. D. Fernández, *Sci. Total Environ.*, 2017, **589**, 11–24.
54 F. Schwab, G. Zhai, M. Kern, A. Turner, J. L. Schnoor and M. R. Wiesner, *Nanotoxicology*, 2016, **10**, 257–278.
55 M. Thapa, R. Sadhukhan, A. Mukherjee and P. K. Biswas, *NanoImpact*, 2023, **29**, 100440.
56 M. Thapa, T. D. Majumdar, C. K. Ghosh, A. Mukherjee and P. K. Biswas, *ACS Food Sci. Technol.*, 2021, **1**, 1595–1604.
57 S. Astolfi, S. Celletti, G. Vigani, T. Mimmo and S. Cesco, *Front. Plant Sci.*, 2021, **12**, 670308.
58 D. Gries, S. Brunn, D. E. Crowley and D. R. Parker, *Plant Soil*, 1995, **172**, 299–308.
59 R. F. H. Giehl and N. von Wirén, *Plant Physiol.*, 2014, **166**, 509–517.
60 B. H. Cheah, Y.-L. Chen, J.-C. Lo, I.-C. Tang, K.-C. Yeh and Y.-F. Lin, *Plant Cell Environ.*, 2021, **44**, 3358–3375.
61 N. P. Evens, P. Buchner, L. E. Williams and M. J. Hawkesford, *Plant J.*, 2017, **92**, 291–304.
62 T. Maharajan, T. P. A. Krishna, S. A. Ceasar and S. Ignacimuthu, *Planta*, 2023, **257**, 44.
63 J. Tiong, G. McDonald, Y. Genc, N. Shirley, P. Langridge and C. Y. Huang, *New Phytol.*, 2015, **207**, 1097–1109.
64 N. Thiébaut and M. Hanikenne, *J. Exp. Bot.*, 2022, **73**, 1699–1716.
65 P. Ahmad, C. A. Jaleel, M. A. Salem, G. Nabi and S. Sharma, *Crit. Rev. Biotechnol.*, 2010, **30**, 161–175.
66 R. Batool, M. J. Umer, B. Hussain, M. Anees and Z. Wang, in *Antioxidant Defense in Plants: Molecular Basis of Regulation*, ed. T. Aftab and K. R. Hakeem, Springer Nature, Singapore, 2022, pp. 157–179.
67 C. Ma, J. C. White, O. P. Dhankher and B. Xing, *Environ. Sci. Technol.*, 2015, **49**, 7109–7122.
68 F. Pejam, Z. O. Ardebili, A. Ladan-Moghadam and E. Danaee, *PLoS One*, 2021, **16**, e0248778.
69 K. Azarin, A. Usatov, T. Minkina, A. Plotnikov, A. Kasyanova, A. Fedorenko, N. Duplii, E. Vechkanov, V. D. Rajput, S. Mandzhieva and S. Alamri, *Chemosphere*, 2022, **287**, 132167.